Using digital repeat photography and eddy covariance data to model grassland phenology and photosynthetic CO2 uptake

Using digital repeat photography and eddy covariance data to model grassland phenology and photosynthetic CO2 uptake

Mirco Migliavacca[a,b,*], Marta Galvagno[b,c], Edoardo Cremonese[c], Micol Rossini[b], Michele Meroni[b,d], Oliver Sonnentag[e], Sergio Cogliati [b], Giovanni Manca[f], Fabrizio Diotri [c], Lorenzo Busetto[b], Alessandro Cescatti[a], Roberto Colombo[b], Francesco Fava[b,g], Umberto Morra di Cella[c], Emiliano Pari [h], Consolata Siniscalco[h], Andrew D. Richardson[e]

[a] European Commission, DG-JRC, Institute for Environment and Sustainability, Climate Change and Air Quality Unit, Ispra, Via Fermi 2749, 21027 Ispra, Italy
[b] Remote Sensing of Environmental Dynamics Laboratory, DISAT, Università degli Studi Milano-Bicocca, Piazza della Scienza 1, 20126 Milan, Italy
[c] Agenzia Regionale per la Protezione dell'Ambiente della Valle d'Aosta, Sez. Agenti Fisici, Aosta, Italy
[d] European Commission, DG-JRC, Institute for Environment and Sustainability, Monitoring Agricultural Resources Unit, Via Fermi 2749, 21027 Ispra, Italy
[e] Department of Organismic and Evolutionary Biology, Harvard University, Cambridge, MA 02138, USA
[f] Institute for Atmospheric Pollution, Consiglio Nazionale delle Ricerche, 87036 Rende, Italy
[g] Desertification Research Group (NRD), Università degli Studi di Sassari, Viale Italia 57, 07100 Sassari, Italy
[h] Plant Biology Department, Università degli Studi di Torino, Viale Pier Andrea Mattioli, 25, 10125 Torino, Italy

a b s t r a c t

The continuous and automated monitoring of canopy phenology is of increasing scientific interest for the multiple implications of vegetation dynamics on ecosystem carbon and energy fluxes. For this purpose we evaluated the applicability of digital camera imagery for monitoring and modeling phenology and physiology of a subalpine grassland over the 2009 and 2010 growing seasons. We tested the relationships between color indices (i.e. the algebraic combinations of RGB brightness levels) tracking canopy greenness extracted from repeated digital images against field measurements of green and total biomass, leaf area index (LAI), greenness visual estimation, vegetation indices computed from continuous spectroradiometric measurements and CO_2 fluxes observed with the eddy covariance technique. A strong relationship was found between canopy greenness and (i) structural parameters (i.e., LAI) and (ii) canopy photosynthesis (i.e. Gross Primary Production; GPP). Color indices were also well correlated with vegetation indices typically used for monitoring landscape phenology from satellite, suggesting that digital repeat photography provides high-quality ground data for evaluation of satellite phenology products. We demonstrate that by using canopy greenness we can refine phenological models (Growing Season Index, GSI) by describing canopy development and considering the role of ecological factors (e.g., snow, temperature and photoperiod) controlling grassland phenology. Moreover, we show that canopy greenness combined with radiation use efficiency (RUE) obtained from spectral indices related to photochemistry (i.e., scaled Photochemical Reflectance Index) or meteorology (i.e., MOD17 RUE) can be used to predict daily GPP. Building on previous work that has demonstrated that seasonal variation in the structure and function of plant canopies can be quantified using digital camera imagery, we have highlighted the potential use of these data for the development and parameterization of phenological and RUE models, and thus point toward an extension of the proposed methodologies to the dataset collected within PhenoCam Network.

1. Introduction

Phenology is the study of the timing of recurring biological events and the causes of their temporal change regarding biotic and abiotic forces (Lieth, 1976). Since the timing of the main plant phenological events and their interannual variability are controlled by meteorological and environmental forcing (e.g. Chuine et al., 2004; Penuelas et al., 2009), phenology has been shown to be an important indicator for the biological impacts of climate change (e.g. IPCC, 2007). The European Alps are assumed to be particularly sensitive to changes in climate (e.g. Beniston, 2005; Rammig et al., 2010), although much uncertainty still exists as to the possible effects of such changes on ecosystems. It is therefore particularly pressing to disentangle the ecological and climatic factors controlling alpine and subalpine grassland phenology, to quantify changes in growing season length and also the effect that phenological changes may have on the ecosystem carbon balance. Some effects of climate change on the Alps have already been observed such as migration of species to higher elevations (Walther et al., 2005) and trends toward longer growing seasons (e.g. Stockli and Vidale, 2004). In particular, the impacts of climate change on alpine and subalpine grasslands will be very likely stronger than on other mountain vegetation because they are highly diverse (Körner, 2005), because of pasture abandonment and the wide range of microclimatic conditions that occur over short distances (e.g. Motta and Nola, 2001; Vittoz et al., 2008; Wohlfahrt et al., 2003; Zeeman et al., 2010).

Most of the studies conducted on the Alps dealing with the development of strategies for long-term phenological monitoring focus on tree species (Ahrends et al., 2008; Busetto et al., 2010; Fonti et al., 2010; Migliavacca et al., 2008; Moser et al., 2010), while only few studies on grassland phenology of the subalpine and alpine belt have been reported (e.g. Cernusca et al., 2008; Fontana et al., 2008; Jonas et al., 2008). This is primarily due to the difficulty in developing a protocol for field observation of grassland phenology focused on the whole canopy and not on a single species.

The relationships between the timing of key phenological events (bud-burst, senescence, etc.), climate and, more recently carbon fluxes have been the subject of intense research, while the relationships between sub-seasonal variations of canopy development and climate have received little attention. The lack of understanding is reflected in the unsatisfactory description of phenology and canopy development in ecosystem models and the resulting, often unrealistic estimation of carbon fluxes. This is particularly true for gross primary production (GPP), which is largely dependent on the accurate description of canopy development (e.g. Kucharik et al., 2006; Migliavacca et al., 2009; Ryu et al., 2008). Thus, we ask how can we more accurately predict and model seasonal canopy development. The use of "near-surface" remote sensing with digital cameras has great potential in improving phenological monitoring because such observations make it possible to collect automated data at high temporal resolution and in a broad range of ecosystems (e.g. Bradley et al., 2010; Garrity et al., 2010; Ryu et al., 2010; Richardson et al., 2009; Sonnentag et al., 2011).

The use of repeated digital images collected by conventional cameras has been shown to be promising for phenological research in various ecosystems including forests (Ahrends et al., 2008, 2009; Graham et al., 2010; Nagai et al., 2010; Richardson et al., 2007, 2009) and arid grasslands (e.g. Kurc and Benton, 2010). In the agricultural field several authors have shown the potential of complete robotic weed control systems based on digital images in achieving a high level of automation (e.g. Slaughter et al., 2008).

However, to the best of our knowledge, there has been no attempt to use these data for the development and optimization of diagnostic and prognostic phenological models. Recently, some phenological models aimed at describing canopy development have been proposed (e.g. Arora and Boer, 2005; Jolly et al., 2005; Choler et al., 2010; Knorr et al., 2010) and few attempts to optimize these models against remotely sensed products have been reported (Stockli et al., 2008; Knorr et al., 2010). Among these models the Growing Season Index (GSI) developed by Jolly et al. (2005) is one of the most increasingly used (e.g. Stockli et al., 2008). GSI is a bioclimatic index that predicts foliar phenology of vegetation throughout the year as a consequence of three drivers: minimum temperature, evaporative demand and daylength.

Furthermore, the direct linkage between observations of canopy greenness through color indices (i.e. the algebraic combinations of RGB brightness levels) obtained from digital camera imagery, CO_2 flux measurements and vegetation indices related to canopy structure (e.g. Normalized Difference Vegetation Index, NDVI (Rouse et al., 1974); MERIS Terrestrial Chlorophyll Index, MTCI (Dash and Curran, 2004)) and functioning (e.g. Photochemical Reflectance Index, PRI (Gamon et al., 1992)) might be useful for several reasons: firstly, in investigating the impact of phenology on carbon sequestration (Piao et al., 2008; Richardson et al., 2010); secondly, in improving the description of carbon fluxes at site level through the use of radiation use efficiency (RUE) models (e.g. Monteith and Unsworth, 1990). RUE models assume that carbon fixation is a linear function of the incident photosynthetically-active radiation absorbed by vegetation (APAR) and RUE, which represents the conversion efficiency of absorbed energy to fixed carbon. The APAR can be described by using vegetation indices related to canopy structure while RUE is estimated from daily meteorology (e.g. Heinsch et al., 2006; Veroustraete et al., 2002) or by using spectral VIs related to photosynthetic efficiency or photochemistry (e.g. Gamon et al., 1992, 1997).
In this paper, we analyze a time series of color indices obtained from digital camera imagery collected over a subalpine grassland during 2009 and 2010 with the primary goal of addressing the following research questions: (i) can we use digital camera imagery to monitor the seasonal canopy development of a subalpine grassland? (ii) Can we use digital camera imagery as additional source of information for improving phenological and RUE models? In order to address these questions we firstly compare color indices against other field measurements (e.g. LAI, green and total biomass), spectral vegetation indices (e.g. NDVI, MTCI, etc.) collected using high resolution spectrometers and against carbon flux measurements collected with the eddy covariance technique. Secondly, we use two years of color indices and meteorology to attest several versions of the GSI model regarding their application over subalpine grasslands. Finally, we combine color indices, meteorology (through the use of RUE models) and spectral vegetation indices (VIs) related to canopy structure, green vegetation biomass (NDVI, MTCI) and to photochemistry (PRI) with the aim of describing the temporal variability of GPP.

2. Material and methods

2.1. Site description

The study site is an abandoned pasture of the subalpine belt composed mainly of matgrass (Nardus stricta, Arnica montana, Trifolium alpinum and Carex sempervirens as dominant species), located at 2160 m a.s.l. (45◦50_40_ N, 7◦34_41_ E), in the North- Western Italian Alps (Aosta Valley – Torgnon). The area is classified as an intra-alpine region with semicontinental climate with an annual mean temperature of 3.1 ◦C and mean annual precipitation of about 920 mm. The snow-free period lasts generally from late May to early November. The 2009 growing season was considerable less rainy than that of 2010 with a total amount of precipitation during the snow-free period of 172 mm and 362 mm respectively.

2.2. Digital camera set-up and image analysis

Canopy images were collected with a Campbell digital camera (model CC640 Campbell Scientific, Logan, UT, USA) installed in a weatherproof enclosure at a height of 2.5 m above the ground. The

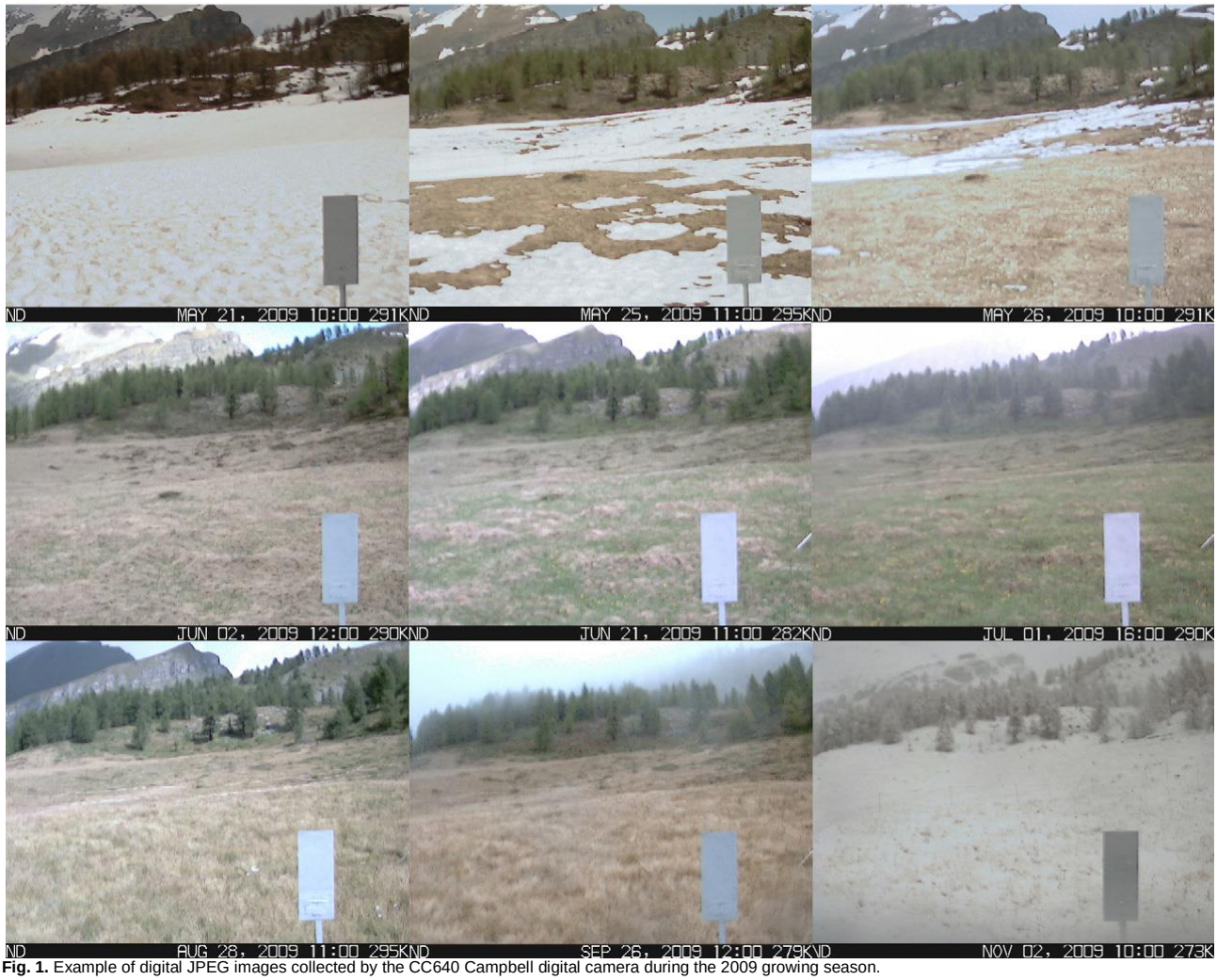

Fig. 1. Example of digital JPEG images collected by the CC640 Campbell digital camera during the 2009 growing season.

camera was pointed north, and set at an angle of about 20◦ below horizontal following Richardson et al. (2007). Camera focal length was 3.5 mm and the field of view was approximately 79.8◦. Because the camera position was fixed, the scene was identical from day to day.

The camera was connected to a CR1000 Campbell data-logger and provided JPEG images of the same scene (resolution 640 × 480, 0.3 megapixels, with three color channels of 8-bit RGB color information, i.e. digital numbers ranging from 0 to 255) every hour from 10 am to 4 pm. The camera–JPEG compression mode was set to "None", to produce the best quality JPEG files with no artifacts from "lossy" compression algorithms.

The camera operated with automatic exposure and aperture mode, responding to ambient light levels using the entire image to adjust the exposure settings. Thus, the brightness of any individual pixel was not a direct measure of surface radiance per se. The camera did not record the exposure setting along with the image, thus preventing the conversion of the images into digital numbers (DN) proportional to radiance.

The present study was based on the analysis of 1940 images recorded between the 21st May 2009 (DOY 141) and the 20th November 2010 (DOY 324). Sample images from throughout the year 2009 are presented in Fig. 1. To minimize the angular effect of the canopy's hemispherical directional reflectance function (Chen et al., 2000) only the images taken from 11 am to 1 pm were used. We developed an R script (R version 2.11.1, R Development Core Team, 2009) to process and analyze the archived digital image files. Analyses were based on time series extracted from one specific "Region of Interest" (ROI) as illustrated in Fig. 2. The dimension of the ROI was selected to provide a reasonably extended spatial sampling of foreground canopy while avoiding the inclusion of the area in the background that might be exposed to different light conditions (e.g. scattered low clouds and fog in the background).

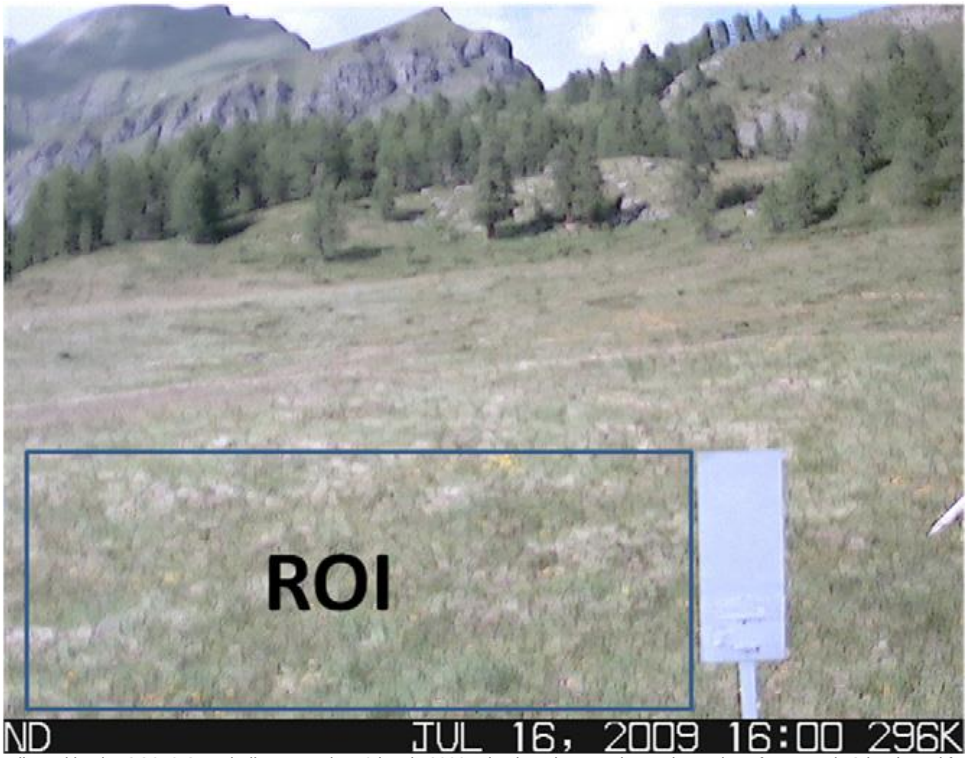

Fig. 2. Digital image collected by the CC640 Campbell camera the 16th July 2009. Blue box denotes the static Region of Interest (ROI) selected for the study. The grey reference panel is visible on the bottom right portion of the image.

The color indices were computed on each archived image: the red, blue and green digital numbers (DN) of each pixel were extracted and averaged over the ROI for each image. Then, the percent of relative brightness (RGB chromatic coordinates in Gillespie et al., 1987) of each channel were computed as in Eqs. (2)–(4) (RI, GI and BI):

$$TotalDN = R_{DN} + G_{DN} + B_{DN} \quad (1)$$

$$RI = \frac{R_{DN}}{TotalDN} \quad (2)$$

$$GI = \frac{G_{DN}}{TotalDN} \quad (3)$$

$$BI = \frac{B_{DN}}{TotalDN} \quad (4)$$

where R_{DN}, G_{DN}, B_{DN} are the red, green and blue DN values of each color channel respectively. As mentioned above, the Campbell CC640 automatically optimizes the exposure time without recording it. Therefore it is not possible to compute the number of digital counts in the unit time, the physical quantity needed to correctly normalize the images for the incident irradiance. The use of RGB chromatic coordinates (Eqs. (2)–(4)) instead of RGB brightness levels suppresses the influence of changes in scene illumination due to cloud cover, solar illumination, as well as image exposure and internal camera processing.

An additional color index, the greenness excess index (GEI, Richardson et al., 2009; Woebbecke et al., 1995), was also computed (Eq. (5)):

$$GEI = 2 \cdot G_{DN} - (R_{DN} - B_{DN})$$

Color indices were computed for the selected ROI for each image. Then, the color indices computed for the three images recorded between 11 am and 1 pm on each day were averaged to get a mean daily value of each color indices. To assess the overall quality of the retrieved signal and the dayto- day stability of the imagery color balance, one ROI from the grey panel (Fig. 2) was extracted. The coefficient of variation of the RGB chromatic coordinates (Eqs. (2)–(4)) during the two growing season was 3.9%, 1.8% and 3.3% for RI, GI and BI respectively, giving us confidence to the quality of the retrieved signal.

Image quality was sometimes adversely affected by rain, snow, aerosols, fog and uneven illumination due to the presence of scattered clouds. The result is that smooth trajectories of the color indices related to canopy greenness were sometimes interrupted by a sharp increase or decrease in VI values, lasting for one or a few days. The time series of daily average color indices were thus filtered to suppress unusual high or low values with a recursive outlier removal filtering. A cubic smoothing spline, with variable degrees of freedom (df) set to the ratio between time series length and 10 (i.e. for time series of 300 days, df was set equal to 30), was fitted to GI and GEI data. Then, the residuals between daily color indices and the smoothing spline were calculated. A particular day was considered as 'good' and then retained for further analysis if the absolute value of the daily residual was less than _ + 3_, where _ is the mean of the residuals and _ is their standard deviation. The algorithm described above was recursively applied to the color indices time series until no outliers were detected (with a maximum of 10 loops). We selected a smoothing spline because it was previously found to be useful to extract phenological patterns from remotely sensed observations (Bradley et al., 2007).

2.3. Eddy covariance flux measurements and micrometeorological data

CO_2, water and energy fluxes between vegetation and atmosphere were measured using the eddy covariance (EC) technique (e.g. Baldocchi et al., 1996). Wind velocity components were measured using a three-dimensional sonic anemometer (CSAT-3 Campbell Scientific Inc., Logan, UT, USA) positioned at a height of 2.5 m above the surface. Water vapor and CO_2 fluctuations were measured with a fast-responding open-path infrared gas analyzer (IRGA, LI-7500, LI-COR Inc., Lincoln NE, USA). Eddy fluxes were calculated with a time step of 30 min according to EUROFLUX methodology (Aubinet et al., 2000).

Along with EC fluxes, the main meteorological variables were measured every 30 min, among these photosynthetically active radiation (PAR), air temperature (T_{Air}) and relative humidity (RH) were measured above the grassland by means of a quantum sensor (LI-190s, LI-COR Inc.) and a shielded thermo-hygrometer (HMP45C, Vaisala Inc., Woburn, MA, USA) respectively. The vapor pressure deficit (VPD) was computed from T_{Air} and RH. Precipitation was measured using a tipping bucket rain gauge (CS700, Campbell Scientific, Logan, UT, USA); soil water content (SWC) was measured with water content reflectometers (CS-616, Campbell Scientific, Logan, UT, USA), installed at two different depths (5–30 cm) while snow height was measured with an ultrasonic distance sensor (SR50, Campbell Scientific, Logan, UT, USA). Day length was computed using potential incoming solar radiation modeled by the r.sun routine (Hofierka and Suri, 2002) implemented in GRASS Open Source GIS (GRASS Development Team, 2008) with a 2-min time step. Day length was computed as the sum of the time steps with potential radiation values higher than 20 W m^{-2}. In order to discard doubtful half-hourly data, in which the theoretical requirements of the eddy covariance technique are not fulfilled, we performed the tests for stationarity and integral turbulent characteristics following Foken and Wichura (1996). Results from integral turbulence and stationarity tests were combined to get the overall quality flag for each half-hour period using the standard procedure followed in Carboeurope-IP project (Mauder and Foken, 2004). Data belonging to class 2 (questionable data quality, gap filling necessary) were discarded.

In order to avoid the possible underestimation of fluxes in stable conditions, data with friction velocity (u*) lower than an appropriate threshold were filtered. A critical u* threshold of 0.050 m s^{-1} was estimated using a procedure similar to Papale et al. (2006). Quality control tests rejected 10.37% of the measured data while data below the critical u* threshold were about 11.37%. In the following analyses, we only used the flux data which passed the above described tests. To assess the consistency of the EC measurements, we analyzed the energy balance closure (Aubinet et al., 2001) by computing the slope of the linear relationship between half-hourly sums of latent heat, sensible heat and their storage, measured with the EC system, and the sums of half-hourly net radiation and soil heat flux obtained with independent methods. The heat storages of biomass and soil were not considered in this analysis. The energy balance closure for the snow-free period in the 2 measurement years was 0.69. For the gap-filling and partitioning of fluxes, the marginal distribution sampling (MDS) method and the partitioning method described in Reichstein et al. (2005), implemented in the online tool (http://www.bgc-jena.mpg.de/bgc-mdi/html/eddyproc/), were used.

2.4. Estimation of flux footprint

The footprint of eddy covariance flux measurements was determined through the analytical model of Schuepp et al. (1990) which measures the cumulative normalized contribution to the surface flux from an upwind source area

The target ecosystem is represented in the area in Fig. 3. Considering all the data belonging to the quality class 0 and 1 (Mauder and Foken, 2004) above the critical u* threshold, the median of the

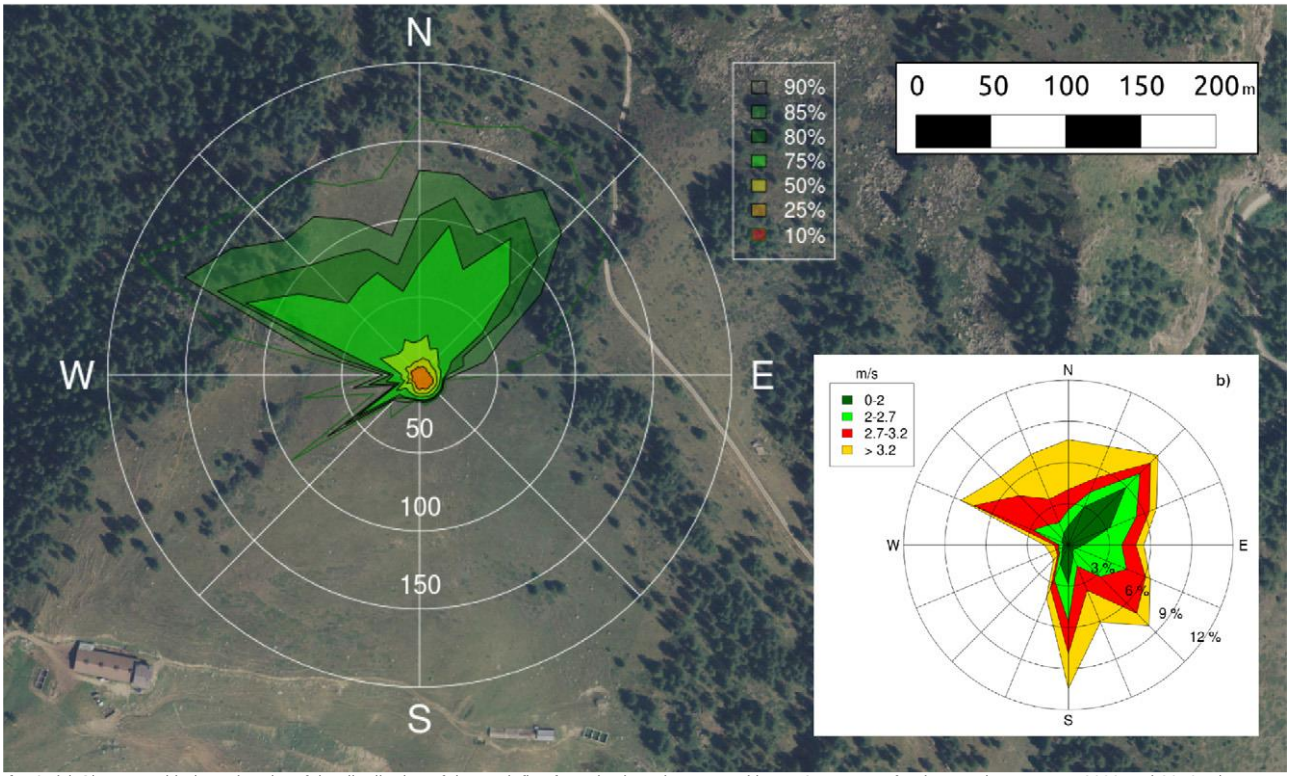

Fig. 3. (a) Site map with the polar plot of the distribution of the peak flux footprint (X_{MAX}) computed by 11.25° sectors for the growing seasons 2009 and 2010. The isolines and different colors represent the percentiles of the distribution of X_{MAX} in a particular sector. (b) Wind rose: wind frequencies are expressed in percentages and computed by 11.5° wind sectors for the growing seasons 2009 and 2010. The colors in each sector indicate the wind speed class. (For interpretation of the references to color in this figure legend, the reader is referred to the web version of the article.)

values of the peak flux footprint (X_{MAX}) was 17.8 m (Fig. 3a). During daytime the median of X_{MAX} was lower (14.23 m). These values are in agreement with other analysis conducted with a similar experimental set-up over alpine grasslands (e.g. Marcolla and Cescatti, 2005). Considering the daytime fluxes about the 90% of the fluxes was emitted by an area within 40 m around the eddy covariance system. The distribution of the X_{MAX} position (Fig. 3) confirmed that the measured scalar flux was representative of the area we are focusing on and that the contribution of fluxes from the target ecosystem is by far dominating the overall budget. 2.5. Ancillary and radiometric measurements During 2009 and 2010 growing seasons additional data on vegetation structure and phenology were periodically collected. Leaf Area Index (LAI), green and total (green and dry) aboveground biomass were measured every two weeks by sampling the phytomass at 12 selected plots of 40 cm×40 cm in the study area.

At each sampling date LAI was estimated at each plot by using a scanning device and the average value was computed. The maximum LAI was reached in July (2.7 $m^2 m^{-2}$ in 2009 and 2.8 $m^2 m^{-2}$ in 2010). In the same 12 plots, visual observations of canopy greenness (greenness visual estimation, GVE) were collected and averaged for the estimation of canopy GVE. Canopy spectral properties were measured with an automatic hyperspectral system named HSI (HyperSpectral Irradiometer) operating in the spectral range 400–1000 nm with a spectral resolution of 1 nm (Meroni et al., 2011; Meroni and Colombo, 2009). HSI was installed at the site and operated continuously for almost the entire growing seasons (130 days in 2009 and 148 days in 2010), collecting spectral signatures of the canopy about every 5 min. Spectral data were used to compute vegetation indices (VIs) related to canopy structure such as the Normalized Difference Vegetation Index (NDVI, Rouse et al., 1974, Eq. (6)) and the MTCI (Meris Terrestrial Chlorophyll Index, Dash and Curran, 2004, Eq. (7)). The Photochemical Reflectance index (PRI, Gamon et al., 1992), related to canopy functioning, was also computed. PRI was scaled (sPRI) according to Rahman et al. (2001) in a range of 0–1 for use as an efficiency factor (Eq. (8)):

$$NDVI = \frac{\rho_{800} - \rho_{600}}{\rho_{800} + \rho_{680}} \quad (6)$$

$$MTCI = \frac{\rho_{753.75} - \rho_{708.75}}{\rho_{708.75} - \rho_{681.25}} \quad (7)$$

$$sPRI = \frac{\left((\rho_{531} - \rho_{570})/(\rho_{531} + \rho_{570}) + 1\right)}{2} \quad (8)$$

where ρ_x is the reflectance computed at the x wavelength in nm. For consistency with color indices, midday VIs (average of all data collected from 11 am to 1 pm) were computed and used for further analyses.

2.6. Using color indices for model development

We assessed the potential for using color indices to develop and parameterize phenological and RUE models.

2.6.1. Growing Season Index (GSI) model

Canopy development was modeled using the GSI (Growing Season Index, Jolly et al., 2005). In its original formulation, GSI assumed that canopy development was driven by three climatic controls: minimum daily temperature T_{MIN} (°C), day length or photoperiod Ph (h) and mean day-light VPD (h Pa). The daily value of GSI was computed as the 21-day running average of the index iGSI. iGSI was calculated daily as the product of three factors (f(T_{MIN}), f(Ph)

Table 1 Summary of different Growing Season Index (GSI) formulations tested (described in Section 2.6.1 in the text). Grey areas represent the environmental factors used by the different model formulations for the calculation of the daily GSI value: f(T_{MIN}) represents the constrain of minimum temperature, f(Ph) represents the day-

length constraint, f(VPD) represents the constraint of vapor pressure deficit (VPD), f(SNOW) represents the constraint due by the presence of snow cover while f(SWC) represents the constraint of the soil water content.

GSI formulation	$f(T_{MIN})$	$f(Ph)$	$f(VPD)$	$f(SNOW)$	$f(SWC)$
GSI					
$GSI_{Ph+SNOW}$					
GSI_{SNOW}					
GSI_{SWC}					
$GSI_{SWC+SNOW+Ph}$					

and f(VPD)) that vary linearly between 0 and 1 as a consequence of the constraining limits. The constraining limits were described by the empirical climate parameters T_{mmax}, T_{mmin}, Ph_{max}, Ph_{min}, VPD_{max}, and VPD_{min} representing maximum and minimum T_{MIN}, Ph and VPD ranges above/below which canopy development is fully constrained or unconstrained. Given the importance of snow cover and SWC in determining the canopy development of subalpine grasslands, we included two additional factors in the model:

• f(SNOW): a flag that assumes a value of 0 when the canopy is covered by snow and 1 during the snow-free period;

• f(SWC): this scalar function was specified as sigmoidal functions (Eq. (9)) constrained to the interval [0,1].

$$f(SWC) = \frac{1}{1 + e^{(\theta_1 - \theta_2 \cdot SWC)}} \qquad (9)$$

Five different model formulations based on different combinations of the limiting factors were then tested (Table 1): GSI as in Jolly et al. (2005) ('GSI'), GSI with f(SNOW) included for the calculation of iGSI ('$GSI_{Ph+SNOW}$'), GSI with f(SNOW) included for the calculation of iGSI in place of f(Ph) ('GSI_{SNOW}'), the 'GSI_{SNOW}' with f(SWC) in place of f(VPD) (i.e. 'GSI_{SWC}') and finally the '$GSI_{Ph+SNOW}$' with f(SWC) in place of f(VPD) (i.e. '$GSI_{SWC+SNOW+Ph}$'). For each model formulation, model parameters (i.e. T_{mmax}, T_{mmin}, Ph_{max}, Ph_{min}, VPD_{max}, VPD_{min}, _1 and _2) were estimated against the daily GI derived from digital camera imagery for the entire observation period (i.e. growing seasons 2009 and 2010). The main aim of this analysis was to test which model formulation was best supported by data at the hand.

To create a continuous time series of GI for the optimization of the GSI we fitted cubic smoothing splines with degrees of freedom (df) set to the ratio between time series length and 10 (i.e. for time series of 300 days, df was set equal to 30). The spline was preferred to well-known growth models (e.g. logistic model) first of all because of the strongly asymmetric (fast spring growth and slow autumn decrease) shape of the retrieved color index (i.e. GI) and second because it was more flexible than a prescribed function. 2.6.2. Radiation use efficiency (RUE) models For modeling canopy functioning we tested two different RUE approaches.

The first was based on the widely used RUE model MOD 17 (Heinsch et al., 2006), which is the algorithm of the MODIS daily photosynthesis product (MOD17). MOD17 is driven by meteorology (air temperature and VPD), PAR and the fraction of absorbed PAR (fAPAR). Here, MOD17 was driven by the GI as a proxy of fAPAR, so that daily GPP (GPP_i) was modeled as in Eq. (10):

$$GPP_i = RUE_{MAX} \cdot (a_0 + a_1 GI) \cdot PAR \cdot f(VDP) f(T_{MIN}) \qquad (10)$$

where RUE_{MAX} is the maximum radiation use efficiency (gC MJ^{-1}); f(T_{MIN}) and f(VPD) varied linearly between 0 and 1 as a consequence of suboptimal temperatures and water availability for photosynthesis, PAR is the incident PAR expressed in MJ m^{-2}, a_1 and a_0 are the coefficients relating GI and fAPAR. RUE_{MAX}, a_1, a_0 and the parameters of f(T_{MIN}) and f(VPD) were estimated against observed daily GPP.

The second approach was based on Rossini et al. (2010) which showed that the midday GPP can be effectively estimated using only PAR and a combination of structural (e.g. NDVI, MTCI) and functionrelated (e.g. sPRI) VIs computed using high resolution spectral data. Here we extended this approach by including the color index (GI) as a descriptor of canopy greenness. We thus investigated whether color indices and spectral VIs could be combined to predict midday GPP, without relying on meteorological data for determining photosynthetic uptake. We tested two different sets of models for the description of midday GPP (Rossini et al., 2010). The first model set (PV, Eq. (11)) assumed that GPP can be estimated with constant RUE and deriving APAR as the product of PAR_i and a linear function of VIs related to the biomass and photosynthetic pigments (i.e. GI, NDVI, MTCI). The second set of models (E, Eq. (12)) assumed that GPP can be estimated by deriving both the absorbed PAR (APAR) and RUE directly from spectral indices. Hence, model set E combined indices related to photosynthetic components of fAPAR (i.e. GI, NDVI, MTCI) with indices related to RUE (sPRI).

$$GPP_i = (a_0 + a_1 PV_i) \cdot PAR_i \quad \text{Model set PV} \qquad (11)$$

$$GPP_i = (a_0 + a_1 sPRI_i) \cdot (a_2 + a_3 PV_i) \cdot PAR_i \quad \text{Model set E} \qquad (12)$$

where GPP_i, PAR_i, PV_i and $sPRI_i$ are the midday GPP, PAR, VI related to photosynthetic fAPAR (i.e. NDVI, MTCI and GI) and sPRI of the i-th DOY, respectively. Model parameters were derived by fitting the model against midday observed GPP.

2.7. Model parameter estimates and evaluation of model performances

Best-fit model parameters were estimated using either simulated annealing (for GSI and MOD17) or the quasi-Newton method (for parameters in Eqs. (11) and (12)), implemented in the R "optim" routine belonging to the R stats package (R, version 2.11.1). For both methods the residual sum of squares between observed and modeled data (RSS) was used as cost function of the optimization. The main fitting statistics (r_2, the root mean square error, RMSE, and the modeling efficiency, EF) between observed and modeled data were computed to evaluate the overall accuracy of fitted models (Janssen and Heuberger, 1995).

To identify the best model supported by data among different GSI formulations and RUE models we computed the Akaike Information Criterion (AIC, Akaike, 1973). The AIC is a useful indicator since it considers the trade-off between model complexity (i.e. number of parameters, p) and maximum likelihood (here calculated as RSS). The lower the AIC, the better is the model considered. AIC essentially balances better model explanatory power against increasing complexity.

3. Results

3.1. Analysis of color indices, CO_2 fluxes, meteorological fluxes and ancillary data

Time series of midday chromatic coordinates (RI, GI and BI) across the ROI computed for the year 2009 show distinct seasonal signals (Fig. 4a). Both RI and BI were more variable from day-to-day than GI. The time series of GI and GEI computed for the growing season 2009 are reported as example in Fig. 4b and c.

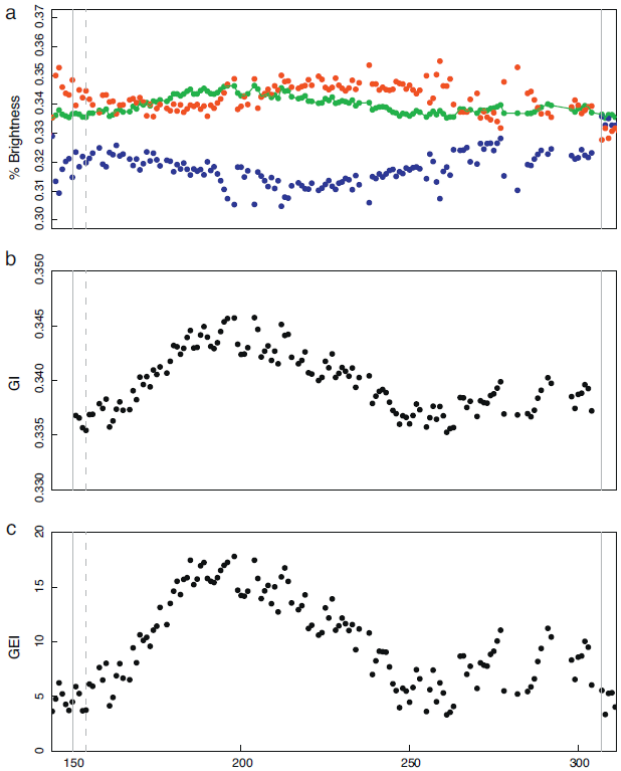

Fig. 4. (a) Time series of relative brightness (% Brightness) of each channel (Eqs. (2)–(4) in the manuscript) for the year 2009: green dots represent greenness indices GI, blue dots blue indices BI, red dots red indices (RI). (b) Time series of Greenness Index, GI (Eq. (2) in the manuscript). (c) Time series of Greenness Excess Index (Eq. (3) in the manuscript). In the x axis the day of the year are reported. Vertical lines highlight the day of snowmelt in spring and snowfall in autumn. Vertical dashed line represent a snowfall event in spring. (For interpretation of the references to color in this figure legend, the reader is referred to the web version of the article.)

The correlation between ancillary data collected in 2009 and 2010 and color indices is reported in Table 2. Results show a positive correlation with green biomass, LAI and GVE, while a not significant correlation was observed with total biomass (dry plus green biomass) indicating that the color indices are not sensitive to dry biomass. A summary of meteorological data, daily GPP and the smoothed time series of GI, GEI, MTCI, NDVI and sPRI for the entire measurement period are reported in Fig. 5. GI was slightly better correlated with the ancillary data than GEI, although the differences were almost negligible. For this reason we further discuss the results only in terms of GI.

Table 2
Pearson's correlation coefficient calculated between ancillary data and color indices computed for the days in which the ancillary data were collected. GI is the Greenness Index, GEI is the Greenness Excess Index, LAI is the Leaf Area Index, GVE is the Green Visual Estimation.

	Total biomass	Green biomass	LAI	GVE
GI	n.s.	0.68*	0.77**	0.72***
GEI	n.s.	0.67*	0.74***	0.70***

* Represent significant correlations ($p < 0.01$).
** Represent significant correlations ($p < 0.001$).
*** Represent significant correlation ($p = 0$), n.s. represents not significant correlation.

GI (Fig. 5d) began rising slowly immediately after the snowmelt (around DOY 150 and 140 for 2009 and 2010, respectively) and at faster rate after DOY 165–170, reaching its maximum at early July (around DOY 190–200 for both years). Over the subsequent weeks, GI showed a steady decline due to autumn yellowing and senescence. In 2009, by DOY 270, however, a pronounced increase in GI was observed (Fig. 5d). Spectral VIs (i.e. NDVI, MTCI) and color indices were in accordance during late spring and early summer (DOY 150–200 in Fig. 5d); although in 2010 both NDVI and MTCI were higher than color indices. In late summer and autumn 2009 and 2010 (around DOY 200–280), MTCI and color indices were again in agreement, although GI was more sensitive to the second greenup in 2009 and also noisier than MTCI. In autumn 2009, sPRI showed an increase that highlighted an increase of photosynthetic activity. NDVI decreased more slowly than color indices and than other VIs. In springtime we observed measurable photosynthetic CO_2 uptake at DOY 150, immediately after snowmelt (Fig. 5c). In both years springtime increases in GPP started synchronous with GI (Fig. 5e), but afterwards GPP tended to lead changes in canopy greenness (GI). During late summer/autumn, canopy development and functioning showed similar responses to meteorological conditions before DOY 250. The increase in GI occurred in autumn 2009 reflected a weaker but detectable increase in GPP (Fig. 5e) in correspondence to a rain pulse (DOY 260–270) and a subsequent increase in SWC (Fig. 5b). Finally, after DOY 306 the snow covered the canopy in both years.

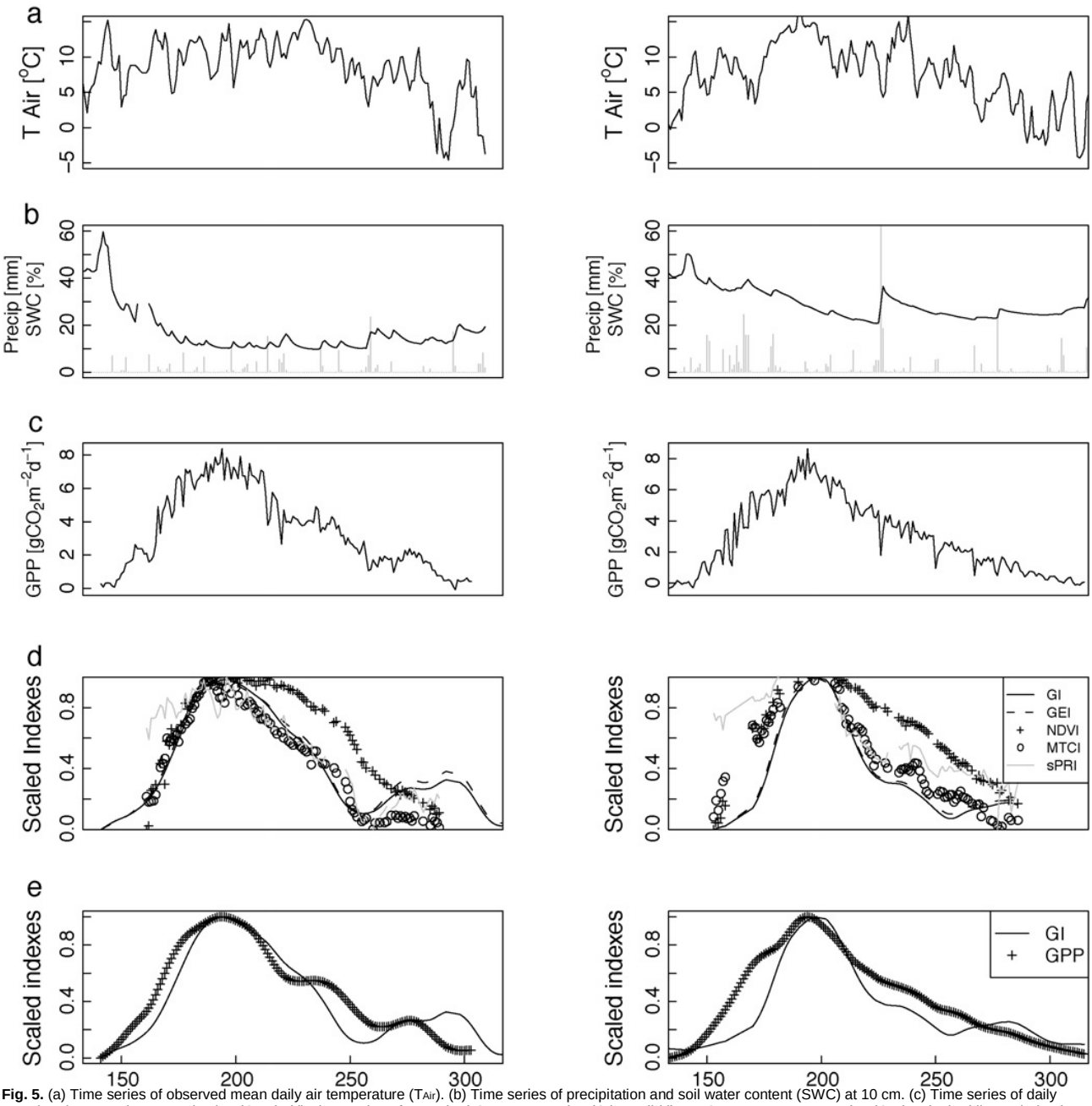

Fig. 5. (a) Time series of observed mean daily air temperature (T_{Air}). (b) Time series of precipitation and soil water content (SWC) at 10 cm. (c) Time series of daily cumulated gross primary production (GPP). (d) Time series of smoothed Greenness Index (GI) – solid line – Greenness Excess Index (GEI) – dashed line – derived from digital camera imagery. Normalized Difference Vegetation Index (NDVI) – crosses – MERIS Terrestrial Chlorophyll Index (MTCI) – dotted and dashed line – and scaled Photochemical Reflectance Index (sPRI) – grey line – computed from spectral signatures collected continuously in the field by the Hyperspectral Irradiometer (HSI). Time series of smoothed Greenness Index (GI) – solid line – and Gross Primary Production (GPP) – crosses (e). The left panel represents 2009 while the right panel is the 2010 growing season.

Correlations between spectral VIs (computed from HSI spectra), GPP and color indices are reported in the correlation matrix in Table 3. MTCI and color indices are strongly correlated (r = 0.82 with GI) while NDVI is less correlated (r = 0.69 with GI).

Table 3
Correlation matrix between color indices derived from digital camera imagery, vegetation indices computed from spectral signatures collected with the Hyperspectral Irradiometer (HSI) and midday Gross Primary Production (GPP). All correlations are significant ($p < 0.01$). GI is the Greenness Index; GEI is the Greenness Excess Index; NDVI is the Normalized Difference Vegetation Index; MTCI is the MERIS Terrestrial Chlorophyll Index.

	NDVI	MTCI	GI	GEI	GPP
NDVI	1	0.87	0.69	0.67	0.83
MTCI		1	0.82	0.80	0.95
GI			1	0.99	0.79
GEI				1	0.78
GPP					1

Table 4
Fitting statistics of the different formulations of Growing Season Index (GSI) model (Table1). MEF is the modeling efficiency, RMSE is the root mean square error, r^2 is the determination coefficient, dAIC is the difference between the Akaike Information Criterion (AIC) computed for the model and the minimum AIC across models (i.e. dAIC of 0 represents the best model formulation). p is the number of model parameters. '$GSI_{SWC+SNOW+Ph}$' (please see description in Section 2.6.1) is the best model according to the AIC criterion, the parameters estimated are: $T_{mmin} = -5.66\,^{\circ}C$, $T_{mmax} = 7.24\,^{\circ}C$, $Ph_{min} = 6.8$ h, $Ph_{max} = 14.71$ h, $\theta_1 = 8.92$ and $\theta_2 = 0.69$.

Model	r^2	MEF	RMSE	dAIC	P
GSI	0.6	0.55	0.20	315.28	6
GSI_{SNOW}	0.59	0.59	0.18	200.85	6
$GSI_{Ph+SNOW}$	0.82	0.80	0.13	42.95	8
$GSI_{SWC+SNOW}$	0.80	0.79	0.14	52.85	6
$GSI_{SWC+SNOW+Ph}$	0.86	0.84	0.12	0	8

3.2. The GSI model

The statistics for the different formulations of the GSI model fitted against the time series of daily GI are reported in Table 4. Despite higher complexity (i.e. a larger number of parameters), the best model selected by AIC was the $GSI_{SWC+SNOW+Ph}$. The $GSI_{SWC+SNOW}$ showed a performance comparable to the best model, while the

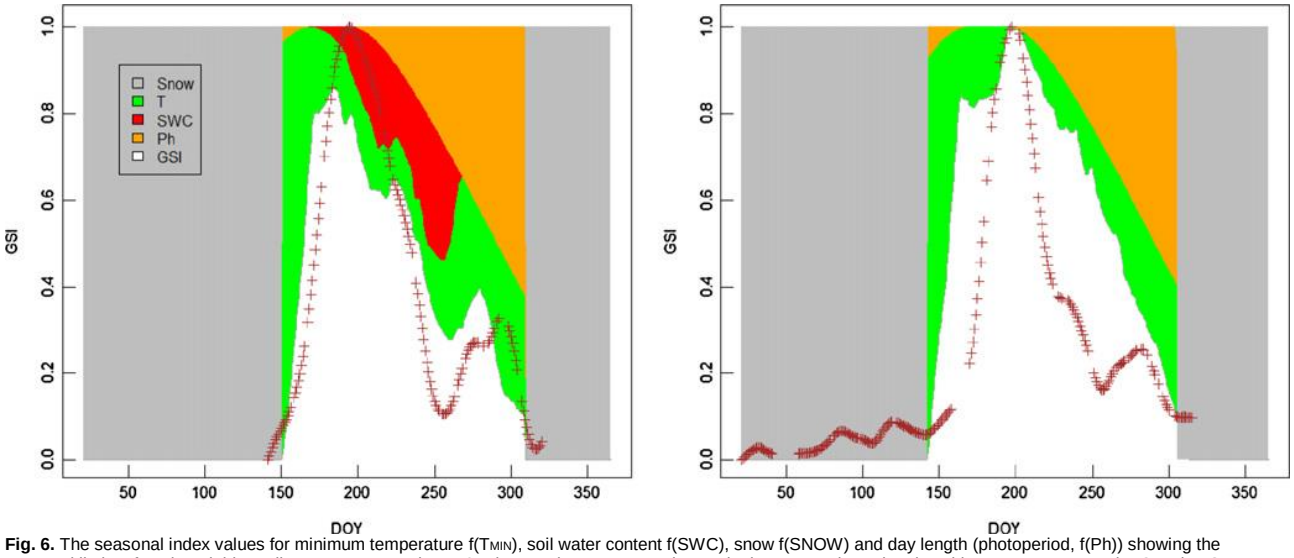

Fig. 6. The seasonal index values for minimum temperature f(T_{MIN}), soil water content f(SWC), snow f(SNOW) and day length (photoperiod, f(Ph)) showing the seasonal limits of each variable. Indices are presented as a 21-day running average to better depict seasonal trends. The white area represents the Growing Season Index (GSI) while crosses represent the Greenness Index (GI) derived from digital camera imagery. The green areas represent the relative importance of temperature as limiting factor, the grey areas represent the limitation due to presence of snow, the orange areas the limitation due to day length while the red area the limitation due to suboptimal soil water content conditions. The left panel represents 2009 while the right panel is the 2010 growing season. (For interpretation of the references to color in this figure legend, the reader is referred to the web version of the article.)

original formulation and the GSI_{SNOW} showed a poorer performance. The time series of $GSI_{SWC+SNOW+Ph}$ is reported in Fig. 6. Individual daily color index values of the relative influence for T_{MIN}, SWC, day length and snow for 2009 and 2010 are shown in Fig. 6. During spring, snow (grey area) and temperatures (green area) were the primary limiting factors while day length was more important in 2010 when the snow-melt occurred before (around DOY 140). Autumn phenology was driven by soil water availability, temperature and photoperiod in 2009 while in 2010 water availability was not a limiting factor.

3.3. Performance of RUE models

Results of the statistical analysis of the performance of the different RUE models showed that color indices (i.e. GI), when combined with meteorology or remotely sensed estimation of RUE can be successfully used for the description of the GPP (Table 5). The MOD17 model results showed that by using meteorology and color indices it was possible to describe the temporal variability of daily GPP quite well (RMSE = 0.87 gC m^{-2} d^{-1}; r^2 = 0.87; EF = 0.85).

Overall, results of model set E (i.e., RUE described by sPRI) were better than those obtained with model set PV (i.e., RUE is constant and GPP is dependent only on VIs related to the presence of photosynthetic material). Results show an improvement in model performances on adding the sPRI, and thus a term related to photosynthetic efficiency, to models driven only by VIs related to canopy structure. According to AIC, the model that used MTCI and sPRI was the best descriptor of daily GPP among the models based on the spectral VIs.

4. Discussion

4.1. Seasonal variations of canopy phenology

This study shows that digital camera imagery are well-suited for monitoring the development and phenology of a subalpine grassland. Color indices derived from these images provide reliable information on canopy status with daily temporal resolution and offer the possibility of continuous and unattended monitoring of timing and rate of canopy development. These achievements are not feasible with traditional phenological observations in such ecosystems, often located in remote areas. This is particularly interesting considering also the current rapid development of webcams and digital cameras, the development of new promising methodologies for monitoring phenology (e.g. Ryu et al., 2010) as well as the development and refining of image processing techniques (e.g. Sonnentag et al., 2011). Moreover, with digital camera imagery we obtained an integrated indicator of canopy development, which is difficult to obtain with traditional phenological campaigns because of the high biodiversity of subalpine grasslands and because the definition of a field protocol for plant phenology is not inconsequential. The ecosystem studied is an interesting test-case for phenological and productivity models because of the fast dynamics of greening, carbon fluxes and physiological activity in response to climatic drivers. As was found by other authors, we observed a strong control of snowfall and snowmelt on phenology (Jonas et al., 2008; Ellebjerg

Table 5
Summary of statistics in fitting (determination coefficient, r^2, root mean square error, RMSE, and Akaike Information Criterion, AIC) of different models tested in this study.GI is the Greenness Index; NDVI is the Normalized Difference Vegetation Index; MTCI is the MERIS Terrestrial Chlorophyll Index (MTCI); sPRI is the scaled Photochemical Reflected Index; RUE_{MAX} is the maximum Radiation Use Efficiency. Model set PV assumed that GPP can be estimated with constant RUE and deriving absorbed photosynthetically active radiation (APAR) as the product of incident PAR and a linear function of vegetation indices related to the biomass and photosynthetic pigments (i.e. GI, NDVI, MTCI). The model set E assumed that GPP can be estimated by deriving both the APAR and RUE directly from remotely sensed data. The best-performing models of PV and E set are in bold print. MOD17 represents the algorithm of the MODIS photosynthesis product (MOD17).

Model set	Driver		r^2	RMSE ($gCm^{-2}\,d^{-1}$)	AIC
	fAPAR	RUE			
PV	GI		0.54	3.01	592.2
	NDVI		0.47	3.22	628.1
	MTCI		**0.58**	**2.85**	563.2
E	GI	sPRI	0.57	2.90	576.4
	NDVI	sPRI	0.59	2.82	561.5
	MTCI	**sPRI**	**0.60**	**2.80**	557.8
MOD17	**GI**	**Meteorology, RUE_{MAX}**	**0.88**	**0.87**	−73.40

et al., 2008): once snow disappeared the canopy suddenly started to sequester carbon and to green-up. The lag observed between these two processes (GPP led GI) was related to the pattern of canopy green-up: matgrass, which is the dominant graminaceous species at the site, starts to green-up from the bottom, below the dry and brown dead biomass of the previous year, thus not completely perceptible by the camera low view angle. Color indices track the increase in canopy greenness only when green starts to be more visible from above. The result of this mechanism was a delay of a few days (6–7 days) between GPP and GI which may have an important influence on the extraction of phenological metrics from the color indices signal.
In 2009, during late summer–autumn, when senescence mechanisms were already active and the canopy was yellowing, two climatic events were observed: a warm week associated with low precipitation first (DOY 225–235) and a rain pulse associated with warmer temperature in late September (Fig. 5a and b from DOY 270). These peculiar conditions allow us to highlight the potential usefulness of digital repeat photography in tracking weekly variations in canopy greenness (Fig. 5d). In fact, the analysis of time courses of color indices showed a rebound of GI that followed the rain pulse and the stimulation of photosynthetic activity highlighted by the concomitant increase in GPP and a more pronounced increase in sPRI. Conversely to spring, in autumn we observed a more rapid decrease in color indices than in GPP. During senescence we observed an increase in dry (and yellow) matter on the top canopy layer which led to a reduction in color indices. However, during this phase there was photosynthetically active vegetation material (i.e. green biomass mainly localized on the bottom of the canopy) which maintained photosynthetic activity as detected by GPP and sPRI.
The effect of the rain pulse in autumn 2009 was to cause a pronounced greening of the canopy detected by the color indices and by MTCI but not by NDVI. In both years autumn MTCI reacts faster than NDVI to variations in chlorophyll content and green biomass due to the fact that the MTCI index is based on wavelengths in the red-edge region which is more sensitive to chlorophyll and green variations (Dash and Curran, 2004). NDVI instead is by far more related to structure, LAI and total biomass. Therefore, NDVI values during autumn were less dynamic and decreased more slowly than MTCI and color indices. NDVI was less able to follow the rapid response of green vegetation and, contrary to MTCI and GI in 2009, did not show any sign of rebound after the rain pulse. The sPRI instead showed a clear rebound in autumn in 2009, thus indicating an increase in RUE as a consequence of the improved meteorological conditions. In fact, sPRI is able to track the interconversion of the xanthophyll cycle pigments in intact leaves (Gamon et al., 1992) and it is increasingly used to assess photosynthetic rates and RUE both at leaf (Gamon et al., 2006; Meroni et al., 2008) and canopy scale (Garbulsky et al., 2008; Hilker et al., 2007, 2010). Jacobs et al. (2009) have shown how a distributed network of digital cameras might be used for phenological monitoring and evaluation of satellite phenological products; our results expand on this work by demonstrating strong correlations between color indices and both the radiometric properties and biological activity of the surface vegetation.

4.2. Using color indices for improving phenological and GPP modeling

The GSI proposed by Jolly et al. (2005) was reformulated for the application to alpine grasslands. The best model selected by the AIC was the one including the occurrence of snow, SWC, day length and minimum temperature as ecological factors controlling canopy development. The accuracy of the models including the VPD and SWC as driver of water availability was almost comparable (i.e. $GSI_{Ph+SNOW}$ and $GSI_{SWC+SNOW+Ph}$ in Table 4). Although the use of SWC is suggested, this result allowed the use of VPD as a surrogate for water availability, as also suggested by Jolly et al. (2005) with the main advantage that VPD is easily computable from temperature for the spatial application of the model.
The main environmental cues controlling the grasslands phenology were snow-melting and temperature during spring with a secondary role of day length. Autumn phenology was the result of the combined effect of cold temperatures and decreasing day length (Fig. 6). However, in 2009, the drier year, water availability played an important role in controlling summer and autumnal canopy development (red area in Fig. 6).
For spring these results are in agreement with other field studies which show that alpine grasslands are primarily limited by temperature and the date of snowmelt (e.g. Larl and Wagner, 2006). During spring we also observed a not negligible role of day length, particularly relevant in 2010 when the snow disappeared earlier in the season. This finding is supported by Keller and Korner (2003) who suggested that several alpine species of grasses are sensitive to photoperiod and may not be able to fully utilize periods of earlier snowmelt. This leads to a rearrangement of community composition in response to warmer and earlier snow-melt (Keller and Korner, 2003). On the basis of our results we then support the hypothesis that any attempts at predicting or modeling future subalpine grass phenology based on warming scenarios needs to account for photoperiod constraints. However, we suggest further analyses to reinforce our results, bearing in mind that they are based on two years of data from a single site.
In terms of model development, we believe that the dates of snow melting in spring and snowfall in autumn have to be included as additional drivers of phenological models for grasslands. In fact, the sole use of photoperiod, as in the original model formulation and in many phenological models, leads to poor performance and an unsatisfactory description of the phenological cycle. For spatial applications the dates of snow presence and snow-melt might be derived from satellite data through the use of the MODIS snowcover product (Hall et al., 2002).

The analysis conducted with RUE models highlighted that GPP can be modeled by combining color indices with meteorological data or spectral VIs related to photosynthetic efficiency. The color indices were strongly related to GPP in spring when variations in photosynthetic rates were largely driven by phenology. Later in the season, the inclusion of predictors of radiation use efficiency was necessary for the description of carbon uptake. For these reasons, although more complex, models including meteorology or sPRI were selected according to the AIC criterion. Considering the models of the class PV, a better description of the GPP was observed using the MTCI and GI rather than the NDVI. This can be explained by the close relation between MTCI and GI and green biomass (Table 2), which controls the energy absorbed by photosynthetic pigments and thus effectively used for photosynthetic processes.
We demonstrate (Fig. 6 and Table 5) that color indices are highly valuable for developing and testing RUE models aimed at the description of GPP and phenological models for the description of the canopy development. These findings point towards a more generic application of the methodology that exploits the time series of color indices collected by the PhenoCam Network (http://klima.sr.unh.edu/). The combination of color indices collected by the network over different biomes and phenological models might help to gain insights into the description of seasonal canopy development. The main implication is the improvement of the poor representation of phenology in process-based or land surface models that might lead to erroneous estimation of carbon fluxes (Kucharik et al., 2006; Migliavacca et al., 2009; Ryu et al., 2008) and biosphere-atmosphere interactions (Abramowitz et al., 2008).

4.3. Uncertainty and limitations in using digital camera imagery
Building on previous work that has demonstrated that seasonal variation in the structure and function of plant canopies can be quantified using digital camera imagery, we have highlighted the potential use of these data for the development and parameterization of phenological and RUE models Nevertheless, some limitations and uncertainties still exist and need to be addressed in order to improve the reliability of the time series of vegetation status derived by RGB color indices (e.g. Sonnentag et al., 2011; Bradley et al., 2010; Richardson et al., 2009; Ide and Oguma, 2010; Ahrends et al., 2008).
These limitations are mainly related to the image quality issue (e.g. digital camera used and experimental set-up), as highlighted by Sonnentag et al. (2011), and to the post processing of color indices (e.g. filtering to minimize variation due to solar elevation and zenith angle, as well as atmospheric conditions). A comparison of the phenological information extracted from different commercial digital cameras installed over the same ecosystem could provide important information about the importance of camera choice (Sonnentag et al., 2010). Moreover, Ide and Oguma (2010) observed firstly a year-to-year drift in color balance and secondly that color balance differed between camera manufacturers. As highlighted by Richardson et al. (2009) and Ide and Oguma (2010), noise in color indices values are due mainly to exposure and weather conditions and can be diminished by setting cameras to fixed white balance rather than to auto white balance. The development of calibration protocols and standards to ensure congruence of long-term data sets from multiple sites is essential.
Another source of uncertainty is related to the post-processing of color indices time series. Different methods for filtering color indices time series, removing questionable daily values due to unfavorable meteorological conditions, might introduce uncertainty for traceability of the canopy seasonal variation and for the extraction of robust phenological metrics (e.g. green-up dates). Here we applied an approach based on a simple outlier removal that worked well at this site. However, in literature other methods ranging from the visual inspection (Ahrends et al., 2008) to the use statistical analysis of pixel brightness or sky color (e.g. Ide and Oguma, 2010), have been proposed. Future efforts should be focused on the development of robust and widely applicable filtering and gap-filling methods (e.g. Sonnentag et al., 2010).
Finally, Richardson et al. (2009) and Ide and Oguma (2010) suggested the use of a grey reference panel placed in the corner of the image for the normalization. Here, we mounted a vertical grey panel and we used the ROI extracted from the grey panel for assessing the overall quality of the retrieved signal and the day-by-day stability of the imagery color balance. However, for the use of the vertical panel for normalization purposes, the different illumination and viewing geometries of canopy and reference panel should be taken into account. This is particularly important over horizontal canopies such as grasslands. In these conditions the different sun-target-sensor and sun-panel-sensor geometries may introduce an additional source of uncertainty and the use of a normalization panel with the same viewing geometry of the target would be preferred. Sonnentag et al. (2011) proposed a promising approach to reconstruct hypothetical horizontal RGB reference that might help to overcome such limitation. Future efforts should be addressed in understanding the correct experimental set-up of the panel over different ecosystems and, in particular, over horizontal canopies. These uncertainties need to be considered, and minimized, to improve long-term phenological monitoring with RGB camera imagery. We showed that color indices can be used to constrain models of canopy phenology and functioning. However, the use of these indices for the analysis of interannual variability (e.g. Sonnentag et al., 2011) and spatial variability (i.e. across site) of canopy structure is still challenging and future efforts should be focused to overcome the uncertainties and limitations discussed above.

5. Summary
The present study shows that digital repeat photography provide reliable information on canopy greenness with a high temporal resolution and can be considered as a useful and relatively low-cost tool for monitoring canopy development of subalpine grasslands. We show that by combining color indices with a refined phenological model able to describe canopy development (GSI) it is possible to identify the main ecological factors controlling subalpine grassland phenology. The main environmental cues identified were snow-melt and temperature during spring while autumn phenology was found to be driven by temperatures, day length and water availability during the drier years. During spring we also observed a significant role of day length particularly relevant when snow-melt occurred earlier (i.e. 2010). This suggests that any attempt at predicting or modeling future alpine plant phenology based on warming scenarios needs to account for photoperiod as additional constraints.
We show that by combining information derived by color indices and meteorological or remotely-sensed information related to photosynthetic efficiency in radiation use efficiency (RUE) scheme it is possible to describe well the temporal variability of carbon uptake.
We conclude that digital camera imagery can provide important information at site level to gain insights into the description of the seasonal canopy development. Digital camera imagery can be consider as a promising tool for testing different models and different hypotheses on the main ecological factors controlling phenology and canopy functioning. However, further work is necessary to overcome limitations related to the image quality issue and processing. In fact, while digital camera imagery are very useful for monitoring the seasonal development of the canopy greenness, a lot uncertainty still exists concerning the use of color indices for monitoring the interannual variability of canopy structural parameters and future efforts should be focused to address this issue.

Acknowledgments
This work was supported by the PhenoALP project, an Interreg project co-funded by the European Regional Development Fund, under the operational program for territorial cooperation Italy–France (ALCOTRA) 2007–2013. MM acknowledges the University of Milano-Bicocca who supported the visiting scientist period at the Harvard University (OEB Department). ADR acknowledges support from the Northeastern States Research Cooperative. We thank the anonymous reviewers for their constructive comments that substantially improved the manuscript. The authors acknowledge Jasper Bloemen for the relevant comments during writing and data analysis; Sara D'Alessandro, Michele Lonati, Giovanni Pavia, Martina Petey, Paolo Pogliotti and Emily Solly for the support during field campaigns.

References

Abramowitz et al., 2008 G. Abramowitz, R. Leuning, M. Clark, A. Pitman Evaluating the performance of land surface models Journal of Climate, 21 (21) (2008), pp. 5468–5481

Ahrends et al., 2008 H.E. Ahrends, R. Brugger, R. Stockli, J. Schenk, P. Michna, F. Jeanneret, H. Wanner, W. Eugster Quantitative phenological observations of a mixed beech forest in northern Switzerland with digital photography Journal of Geophysical Research: Biogeosciences, 113 (2008) G4

Ahrends et al., 2009 H.E. Ahrends, S. Etzold, W.L. Kutsch, R. Stoeckli, R. Bruegger, F. Jeanneret, H. Wanner, N. Buchmann, W. Eugster Tree phenology and carbon dioxide fluxes: use of digital photography at for process-based interpretation the ecosystem scale Climate Research, 39 (3) (2009), pp. 261–274

Akaike, 1973 H. Akaike Information theory and an extension of the maximum likelihood principle B.N. Petrov, F. Csaki (Eds.), Proceedings of the Second International Symposium on Information Theory, Akademiai Kiado, Budapest (1973), pp. 267–281 (Reproduced in Kotz, S., Johnson, N.L., 2003. Breakthroughs in Statistics, vol. I, Foundations and Basic Theory. Springer-Verlag, New York, pp. 610–624)

Arora and Boer, 2005 V.K. Arora, G.J. Boer A parameterization of leaf phenology for the terrestrial ecosystem component of climate models Global Change Biology, 11 (1) (2005), pp. 39–59

Aubinet et al., 2000 M. Aubinet, A. Grelle, A. Ibrom, U. Rannik, J. Moncrieff, T. Foken, A.S. Kowalski, P.H. Martin, P. Berbigier, C. Bernhofer, R. Clement, J. Elbers, A. Granier, T. Grunwald, K. Morgenstern, K. Pilegaard, C. Rebmann, W. Snijders, R. Valentini, T. Vesala Estimates of the annual net carbon and water exchange of forests: the EUROFLUX methodology Advances in Ecological Research, 30 (30) (2000), pp. 113–175

Aubinet et al., 2001 M. Aubinet, B. Chermanne, M. Vandenhaute, B. Longdoz, M. Yernaux, E. Laitat Long term carbon dioxide exchange above a mixed forest in the Belgian Ardennes Agricultural and Forest Meteorology, 108 (4) (2001), pp. 293–315

Baldocchi et al., 1996 D Baldocchi, R. Valentini, S. Running, W. Oechel, R. Dahlman Strategies for measuring and modelling carbon dioxide and water vapour fluxes over terrestrial ecosystems Global Change Biology, 2 (3) (1996), pp. 159–168

Beniston, 2005 M. Beniston Mountain climates and climatic change: an overview of processes focusing on the European Alps Pure and Applied Geophysics, 162 (8–9) (2005), pp. 1587–1606

Bradley et al., 2007 B.A Bradley, R.W. Jacob, J.F. Hermance, J.F. Mustard A curve fitting procedure to derive inter-annual phenologies from time series of noisy satellite NDVI data Remote Sensing of Environment, 106 (2) (2007), pp. 137–145

Bradley et al., 2010 E. Bradley, D. Roberts, C. Still Design of an image analysis website for phenological and meteorological monitoring Environmental Modelling and Software, 25 (1) (2010), pp. 107–116

Busetto et al., 2010 L. Busetto, R. Colombo, M. Migliavacca, E. Cremonese, M. Meroni, M. Galvagno, M. Rossini, C. Siniscalco, U. Morra Di Cella, E. Pari Remote sensing of larch phenological cycle and analysis of relationships with climate in the Alpine region Global Change Biology, 16 (9) (2010), pp. 2504–2517

Cernusca et al., 2008 A. Cernusca, M. Bahn, F. Berninger, U. Tappeiner, G. Wohlfahrt Effects of land-use changes on sources, sinks and fluxes of carbon in European Mountain Grasslands: preface Ecosystems, 11 (8) (2008), pp. 1335–1337

Chen et al., 2000 J.M. Chen, X. Li, T. Nilsonn, A. Strahler Recent advances in geometrical optical modelling and its applications Remote Sensing Review, 18 (2000), pp. 227–262

Choler et al., 2010 P. Choler, W. Sea, P. Briggs, M. Raupach, R. Leuning A simple ecohydrological model captures essentials of seasonal leaf dynamics in semi-arid tropical grasslands Biogeosciences, 7 (3) (2010), pp. 907–920

Chuine et al., 2004 I. Chuine, P. Yiou, N. Viovy, B. Seguin, V. Daux, E.L. Ladurie Historical phenology: grape ripening as a past climate indicator Nature, 432 (7015) (2004), pp. 289–290

Dash and Curran, 2004 J. Dash, P.J. Curran The MERIS terrestrial chlorophyll index International Journal of Remote Sensing, 25 (23) (2004), pp. 5403–5413

Ellebjerg et al., 2008 S.M. Ellebjerg, M.P. Tamstorf, L. Illeris, A. Michelsen, B.U. Hansen Inter-annual variability and controls of plant phenology and productivity at Zackenberg Advances in Ecological Research, Academic Press (2008) pp. 249–273

Foken and Wichura, 1996 T. Foken, B. Wichura Tools for quality assessment of surface-based flux measurements Agricultural and Forest Meteorology, 78 (1–2) (1996), pp. 83–105

Fontana et al., 2008 F Fontana, C. Rixen, T. Jonas, G. Aberegg, S. Wunderle Alpine grassland phenology as seen in AVHRR, VEGETATION, and MODIS NDVI time series – a comparison with in situ measurements Sensors, 8 (4) (2008), pp. 2833–2853

Fonti et al., 2010 P. Fonti, G. von Arx, I. Garcia-Gonzalez, B. Eilmann, U. Sass-Klaassen, H. Gartner, D. Eckstein Studying global change through investigation of the plastic responses of xylem anatomy in tree rings New Phytologist, 185 (1) (2010), pp. 42–53

Gamon et al., 1992 J.A. Gamon, J. Peñuelas, C.B. Field A narrow-waveband spectral index that tracks diurnal changes in photosynthetic efficiency Remote Sensing of Environment, 41 (1) (1992), pp. 35–44

Gamon et al., 2006 J.A. Gamon, A.F. Rahman, J.L. Dungan, M. Schildhauer, K.F. Huemmrich Spectral Network (SpecNet) – what is it and why do we need it? Remote Sensing of Environment, 103 (3) (2006), pp. 227–235

Gamon et al., 1997 J.A. Gamon, L. Serrano, J.S. Surfus The photochemical reflectance index: an optical indicator of photosynthetic radiation use efficiency across species, functional types, and nutrient levels Oecologia, 112 (4) (1997), pp. 492–501

Garbulsky et al., 2008 M.F. Garbulsky, J. Penuelas, D. Papale, I. Filella Remote estimation of carbon dioxide uptake by a Mediterranean forest Global Change Biology, 14 (12) (2008), pp. 2860–2867

Garrity et al., 2010 S.R. Garrity, L.A. Vierling, K. Bickford A simple filtered photodiode instrument for continuous measurement of narrowband NDVI and PRI over vegetated canopies Agricultural and Forest Meteorology, 150 (3) (2010), pp. 489–496

Gillespie et al., 1987 A.R Gillespie, A.B. Kahle, R.E. Walter Color enhancement of highly correlated images. II. Channel ratio and “chromaticity” transformation techniques Remote Sensing of Environment, 22 (1987), pp. 343–365

Graham et al., 2010 E.A. Graham, E.C. Riordan, E.M. Yuen, D. Estrin, P.W. Rundel Public Internet-connected cameras used as a cross-continental ground-based plant phenology monitoring system Global Change Biology, 16 (11) (2010), pp. 3014–3023

GRASS Development Team Geographic Resources Analysis Support System (GRASS) Software. Open Source Geospatial Foundation Project GRASS Development Team (2008)

Hall et al., 2002 D.K. Hall, G.A. Riggs, V.V. Salomonson, N.E. Di Girolamo, K.J. Bayr MODIS snow-cover products Remote Sensing of Environment, 83 (2002), pp. 181–194 |

Heinsch et al., 2006 F.A. Heinsch, M.S. Zhao, S.W. Running, J.S. Kimball, R.R. Nemani, K.J. Davis, P.V. Bolstad, B.D. Cook, A.R. Desai, D.M. Ricciuto, B.E. Law, W.C. Oechel, H. Kwon, H.Y. Luo, S.C. Wofsy, A.L. Dunn, J.W. Munger, D.D. Baldocchi, L.K. Xu, D.Y. Hollinger, A.D. Richardson, P.C. Stoy, M.B.S. Siqueira, R.K. Monson, S.P. Burns, L.B. Flanagan Evaluation of remote sensing based terrestrial productivity from MODIS using regional tower eddy flux network observations IEEE Transactions on Geoscience and Remote Sensing, 44 (7) (2006), pp. 1908–1925

Hilker et al., 2007 T. Hilker, N.C. Coops, Z. Nesic, M.A. Wulder, A.T. Black Instrumentation and approach for unattended year round tower based measurements of spectral reflectance Computers and Electronics in Agriculture, 56 (1) (2007), pp. 72–84

Hilker et al., 2010 T Hilker, F.G. Hall, N.C. Coops, A. Lyapustin, Y. Wang, Z. Nesic, N. Grant, T.A. Black, M.A. Wulder, N. Kljun, C. Hopkinson, L. Chasmer Remote sensing of photosynthetic light-use efficiency across two forested biomes: spatial scaling Remote Sensing of Environment, 114 (12) (2010), pp. 2863–2874

Hofierka and Suri, 2002 J. Hofierka, M. Suri The solar radiation model for Open source GIS: implementation and application M. Ciolli, P. Zatelli (Eds.), Open Source Free Software GISS – GRASS Users Conference (2002)

Ide and Oguma, 2010 R. Ide, H. Oguma Use of digital cameras for phenological observations Ecological Informatics, 5 (5) (2010), pp. 339–347

IPCC, 2007 IPCC Climate Change 2007: synthesis report IPCC, Geneva, Switzerland (2007)

Jacobs et al., 2009 N. Jacobs, W. Burgin, N. Fridrich, A. Abrams, K. Miskell, B.H. Braswell, A.D. Richardson, P. Pless The Global Network of Outdoor Webcams: Properties and Applications ACM GIS’09, Seattle, WA, USA (2009)

Janssen and Heuberger, 1995 P.H.M. Janssen, P.S.C. Heuberger Calibration of process-oriented models Ecological Modelling, 83 (1–2) (1995), pp. 55–66

Jolly et al., 2005 W.M. Jolly, R. Nemani, S.W. Running A generalized, bioclimatic index to predict foliar phenology in response to climate Global Change Biology, 11 (4) (2005), pp. 619–632

Jonas et al., 2008 T. Jonas, C. Rixen, M. Sturm, V. Stoeckli How alpine plant growth is linked to snow cover and climate variability Journal of Geophysical Research: Biogeosciences, 113 (2008) G3

Keller and Korner, 2003 F. Keller, C. Korner The role of photoperiodism in alpine plant development Arctic, Antarctic, and Alpine Research, 35 (3) (2003), pp. 361–368

Knorr et al., 2010 W. Knorr, T. Kaminski, M. Scholze, N. Gobron, B. Pinty, R. Giering, P.P. Mathieu Carbon cycle data assimilation with a generic phenology model Journal of Geophysical Research G: Biogeosciences, 115 (2010), p. G04017

Körner, 2005 C. Körner The green cover of mountains in a changing environment U.M. Huber, H. Bugmann, R. M (Eds.), Global Change and Mountain Regions. An Overview of Current Knowledge, Springer, Berlin (2005)

Kucharik et al., 2006 C.J. Kucharik, C.C. Barford, M. El Maayar, S.C. Wofsy, R.K. Monson, D.D. Baldocchi A multiyear evaluation of a Dynamic Global Vegetation Model at three AmeriFlux forest sites: vegetation structure, phenology, soil temperature, and CO2 and H2O vapor exchange Ecological Modelling, 196 (1–2) (2006), pp. 1–31

Kurc and Benton, 2010 S.A. Kurc, L.M. Benton Digital image-derived greenness links deep soil moisture to carbon uptake in a creosotebush-dominated shrubland Journal of Arid Environments, 74 (5) (2010), pp. 585–594

Larl and Wagner, 2006 I. Larl, J. Wagner Timing of reproductive and vegetative development in Saxifraga oppositifolia in an alpine and a subnival climate Plant Biology, 8 (1) (2006), pp. 155–166

Lieth, 1976 H.H. Lieth Contributions to phenology seasonality research International Journal of Biometeorology, 20 (3) (1976), pp. 197–199

Mauder and Foken, 2004 Mauder, M., Foken, T., 2004. Documentation and instruction manual of the eddy covariance software package TK2. Work Report University of Bayreuth, Dept. of Micrometeorology, 44, 26, ISSN: 1614-8916.

Marcolla and Cescatti, 2005 B. Marcolla, A. Cescatti Experimental analysis of flux footprint for varying stability conditions in an alpine meadow Agricultural and Forest Meteorology, 135 (1–4) (2005), pp. 291–301

Meroni et al., 2011 M. Meroni, A. Barducci, S. Cogliati, F. Castagnoli, M. Rossini, L. Busetto, M. Migliavacca, E. Cremonese, M. Galvagno, R. Colombo The HyperSpectral Irradiometer HSI, a new instrument for long-term and unattended field spectroscopy measurements Review of Scientific Instruments, 82 (4) (2011), pp. 043106–043115

Meroni and Colombo, 2009 M. Meroni, R. Colombo 3S: a novel program for field spectroscopy Computers & Geosciences, 35 (2009), pp. 1491–1496

Meroni et al., 2008 M. Meroni, V. Picchi, M. Rossini, S. Cogliati, C. Panigada, C. Nali, G. Lorenzini, R. Colombo Leaf level early assessment of ozone injuries by passive fluorescence and PRI International Journal of Remote Sensing, 29 (17) (2008), pp. 5409–5422

Migliavacca et al., 2008 M. Migliavacca, E. Cremonese, R. Colombo, L. Busetto, M. Galvagno, L. Ganis, M. Meroni, E. Pari, M. Rossini, C. Siniscalco, U.M. di Cella European larch phenology in the Alps: can we grasp the role of ecological factors by combining field observations and inverse modelling? International Journal of Biometeorology, 52 (7) (2008), pp. 587–605

Migliavacca et al., 2009 M. Migliavacca, M. Meroni, L. Busetto, R. Colombo, T. Zenone, G. Matteucci, G. Manca, G. Seufert Modeling gross primary production of agro-forestry ecosystems by assimilation of satellite-derived information in a process-based model Sensors, 9 (2) (2009), pp. 922–942

Monteith and Unsworth, 1990 J.L. Monteith, M.H. Unsworth Principles of environmental physics (2nd ed.)Edward Arnold, London, United Kingdom (1990) p. 291

Moser et al., 2010 L. Moser, P. Fonti, U. Buntgen, J. Esper, J. Luterbacher, J. Franzen, D. Frank Timing and duration of European larch growing season along altitudinal gradients in the Swiss Alps Tree Physiology, 30 (2) (2010), pp. 225–233

Motta and Nola, 2001 R. Motta, P. Nola Growth trends and dynamics in sub-alpine forest stands in the Varaita Valley (Piedmont, Italy) and their relationships with human activities and global change Journal of Vegetation Science, 12 (2) (2001), pp. 219–230

Nagai et al., 2010 S. Nagai, K.N. Nasahara, H. Muraoka, T. Akiyama, S. Tsuchida Field experiments to test the use of the normalized-difference vegetation index for phenology detection Agricultural and Forest Meteorology, 150 (2) (2010), pp. 152–160

Papale et al., 2006 D Papale, M. Reichstein, M. Aubinet, E. Canfora, C. Bernhofer, W. Kutsch, B. Longdoz, S. Rambal, R. Valentini, T. Vesala, D. Yakir Towards a standardized processing of Net Ecosystem Exchange measured with eddy covariance technique: algorithms and uncertainty estimation Biogeosciences, 3 (4) (2006), pp. 571–583

Penuelas et al., 2009 J. Penuelas, T. Rutishauser, I. Filella Phenology Feedbacks on Climate Change Science, 324 (5929) (2009), pp. 887–888

Piao et al., 2008 S. Piao, P. Ciais, P. Friedlingstein, P. Peylin, M. Reichstein, S. Luyssaert, H. Margolis, J. Fang, A. Barr, A. Chen, A. Grelle, D.Y. Hollinger, T. Laurila, A. Lindroth, A.D. Richardson, T. Vesala Net carbon dioxide losses of northern ecosystems in response to autumn warming Nature, 451 (7174) (2008), pp. 49–52

R, 2009 R Development Core Team R: A Language and Environment for Statistical Computing R Foundation for Statistical Computing, Vienna (2009) ISBN: 3-900051-07-0, http://www.R-project.org

Rahman et al., 2001 A.F. Rahman, J.A. Gamon, D.A. Fuentes, D.A. Roberts, D. Prentiss Modeling spatially distributed ecosystem flux of boreal forest using hyperspectral indices from AVIRIS imagery J. Geophys. Res., 106 (D24) (2001), pp. 33579–33591

Rammig et al., 2010 A. Rammig, T. Jonas, N.E. Zimmermann, C. Rixen Changes in alpine plant growth under future climate conditions Biogeosciences, 7 (6) (2010), pp. 2013–2024

Reichstein et al., 2005 M. Reichstein, E. Falge, D. Baldocchi, D. Papale, M. Aubinet, P. Berbigier, C. Bernhofer, N. Buchmann, T. Gilmanov, A. Granier, T. Grunwald, K. Havrankova, H. Ilvesniemi, D. Janous, A. Knohl, T. Laurila, A. Lohila, D. Loustau, G. Matteucci, T. Meyers, F. Miglietta, J.M. Ourcival, J. Pumpanen, S. Rambal, E. Rotenberg, M. Sanz, J. Tenhunen, G. Seufert, F. Vaccari, T. Vesala, D. Yakir, R. Valentini On the separation of net ecosystem exchange into assimilation and ecosystem respiration: review and improved algorithm Global Change Biology, 11 (9) (2005), pp. 1424–1439

Richardson et al., 2010 A.D. Richardson, T.A. Black, P. Ciais, N. Delbart, M.A. Friedl, N. Gobron, D.Y. Hollinger, W.L. Kutsch, B. Longdoz, S. Luyssaert, M. Migliavacca, L. Montagnani, J.W. Munger, E. Moors, S.L. Piao, C. Rebmann, M. Reichstein, N. Saigusa, E. Tomelleri, R. Vargas, A. Varlagin Influence of spring and autumn phenological transitions on forest ecosystem productivity Philosophical Transactions of the Royal Society B: Biological Sciences, 365 (1555) (2010), pp. 3227–3246

Richardson et al., 2009 A.D. Richardson, B.H. Braswell, D.Y. Hollinger, J.P. Jenkins, S.V. Ollinger Near-surface remote sensing of spatial and temporal variation in canopy phenology Ecological Applications, 19 (6) (2009), pp. 1417–1428

Richardson et al., 2007 A.D. Richardson, J.P. Jenkins, B.H. Braswell, D.Y. Hollinger, S.V. Ollinger, M.L. Smith Use of digital webcam images to track spring green-up in a deciduous broadleaf forest Oecologia, 152 (2) (2007), pp. 323–334

Rossini et al., 2010 M. Rossini, M. Meroni, M. Migliavacca, G. Manca, S. Cogliati, L. Busetto, V. Picchi, A. Cescatti, G. Seufert, R. Colombo High resolution field spectroscopy measurements for estimating gross ecosystem production in a rice field Agricultural and Forest Meteorology, 150 (9) (2010), pp. 1283–1296

Rouse et al., 1974 J.W. Rouse, R.H. Haas, J.A. Schell, D.W. Deering, J.C. Harlan (Eds.), Monitoring the Vernal Advancements and Retro Gradation of Natural Vegetation, Greenbelt, MD, USA (1974)

Ryu et al., 2008 S.R. Ryu, J. Chen, A. Noormets, M.K. Bresee, S.V. Ollinger Comparisons between PnET-Day and eddy covariance based gross ecosystem production in two Northern Wisconsin forests Agricultural and Forest Meteorology, 148 (2) (2008), pp. 247–256

Ryu et al., 2010 Y. Ryu, D.D. Baldocchi, J. Verfaillie, S. Ma, M. Falk, I. Ruiz-Mercado, T. Hehn, O. Sonnentag Testing the performance of a novel spectral reflectance sensor, built with light emitting diodes (LEDs), to monitor ecosystem metabolism, structure and function Agricultural and Forest Meteorology, 150 (12) (2010), pp. 1597–1606

Schuepp et al., 1990 P.H. Schuepp, M.Y. Leclerc, M.Y. MacPherson, R.L. Desjardins Footprint prediction of scalar fluxes from analytical solutions of the diffusion equation Boundary–Layer Meteorology, 50 (1) (1990), pp. 355–373

Slaughter et al., 2008 D.C. Slaughter, D.K. Giles, D. Downey Autonomous robotic weed control systems: a review Computers and Electronics in Agriculture, 61 (1) (2008), pp. 63–78

Sonnentag et al., 2010 Sonnentag, O., Hufkens, K., Teshera-Sterne, C., Young, A.M., Richardson, A.D., 2010. Phenological research using digital image archives: how important is camera system choice? Abstract B41C-0324 presented at 2010 Fall Meeting, AGU, San Francisco, Calif., 13–17 Dec.

Sonnentag et al., 2011 O. Sonnentag, M. Detto, R. Vargas, Y. Ryu, B.R.K. Runkle, M. Kelly, D.D. Baldocchi Tracking the structural and functional development of a perennial pepperweed (Lepidium latifolium L.) infestation using a multi-year archive of webcam imagery and eddy covariance measurements Agricultural and Forest Meteorology, 151 (2011), pp. 916–926

Stockli et al., 2008 R. Stockli, T. Rutishauser, D. Dragoni, J. O'Keefe, P.E. Thornton, M. Jolly, L. Lu, A.S. Denning Remote sensing data assimilation for a prognostic phenology model Journal of Geophysical Research: Biogeosciences, 113 (2008) G4

Stockli and Vidale, 2004 R. Stockli, P.L. Vidale European plant phenology and climate as seen in a 20-year AVHRR land-surface parameter dataset International Journal of Remote Sensing, 25 (17) (2004), pp. 3303–3330

Veroustraete et al., 2002 F. Veroustraete, H. Sabbe, H. Eerens Estimation of carbon mass fluxes over Europe using the C-Fix model and Euroflux data Remote Sensing of Environment, 83 (3) (2002), pp. 376–399

Vittoz et al., 2008 P. Vittoz, J. Bodin, S. Ungricht, C. Burga, G.R. Walther One century of vegetation change on Isla Persa, a nunatak in the Bernina massif in the Swiss Alps Journal of Vegetation Science, 19 (5) (2008), pp. 671–728

Walther et al., 2005 G.R. Walther, S. Beissner, C.A. Burga Trends in the upward shift of alpine plants Journal of Vegetation Science, 16 (5) (2005), pp. 541–548

Woebbecke et al., 1995 D.M. Woebbecke, G.E. Meyer, K. VonBargen, D.A. Mortensen Color indices for weed identification under various soil, residue, and lightning conditions Transactions of the ASAE (American Society of Agricultural Engineers), 38 (1995), pp. 259–269

Wohlfahrt et al., 2003 G. Wohlfahrt, M. Bahn, C. Newesely, S. Sapinsky, U. Tappeiner, A. Cernusca Canopy structure versus physiology effects on net photosynthesis of mountain grasslands differing in land use Ecological Modelling, 170 (2–3) (2003), pp. 407–426

Zeeman et al., 2010 M.J. Zeeman, R. Hiller, A.K. Gilgen, P. Michna, P. Pluss, N. Buchmann, W. Eugster Management and climate impacts on net CO2 fluxes and carbon budgets of three grasslands along an elevational gradient in Switzerland Agricultural and Forest Meteorology, 150 (4) (2010), pp. 519–530